

LA-UR- 98-3755

Approved for public release;
distribution is unlimited.

Title: FIRST RESULTS FOR A SUPERCONDUCTING
IMAGING-SURFACE SENSOR ARRAY FOR
MAGNETOENCEPHALOGRAPHY

CONF-980899--

Author(s): Robert H. Kraus, Jr., Edward R. Flynn,
Michelle A. Espy, Andrei Matlachov,
William Overton, Charles C. Wood, Mark
V. Peters, and Patrick Ruminer, P-21
Biophysics Group

Submitted to: Proceedings for the Biomag 98
Conference, Sendai, Japan, August 28 -
September 2, 1998

RECEIVED
MAY 03 1999
OSTI

DISTRIBUTION OF THIS DOCUMENT IS UNLIMITED

MASTER

Los Alamos
NATIONAL LABORATORY

Los Alamos National Laboratory, an affirmative action/equal opportunity employer, is operated by the University of California for the U.S. Department of Energy under contract W-7405-ENG-36. By acceptance of this article, the publisher recognizes that the U.S. Government retains a nonexclusive, royalty-free license to publish or reproduce the published form of this contribution, or to allow others to do so, for U.S. Government purposes. Los Alamos National Laboratory requests that the publisher identify this article as work performed under the auspices of the U.S. Department of Energy. The Los Alamos National Laboratory strongly supports academic freedom and a researcher's right to publish; as an institution, however, the Laboratory does not endorse the viewpoint of a publication or guarantee its technical correctness.

DISCLAIMER

This report was prepared as an account of work sponsored by an agency of the United States Government. Neither the United States Government nor any agency thereof, nor any of their employees, makes any warranty, express or implied, or assumes any legal liability or responsibility for the accuracy, completeness, or usefulness of any information, apparatus, product, or process disclosed, or represents that its use would not infringe privately owned rights. Reference herein to any specific commercial product, process, or service by trade name, trademark, manufacturer, or otherwise does not necessarily constitute or imply its endorsement, recommendation, or favoring by the United States Government or any agency thereof. The views and opinions of authors expressed herein do not necessarily state or reflect those of the United States Government or any agency thereof.

DISCLAIMER

Portions of this document may be illegible in electronic image products. Images are produced from the best available original document.

First Results for a Superconducting Imaging-Surface Sensor Array for Magnetoencephalography

R.H. Kraus, Jr., E.R. Flynn, W. Overton, M.A. Espy, J.S. George, A. Matlachov,
M.V. Peters, and P. Ruminer

Los Alamos National Laboratory, Los Alamos, New Mexico, 87545

Introduction

Magnetoencephalography (MEG) follows from the initial fundamental work of Cohen[1] in 1968 and development by several groups, most notably at MIT[2] and at NYU[3], based on the development of the Superconducting QUantum Interference Device (SQUID) using the Josephson effect[4]. The SQUID's incredible sensitivity to magnetic fields permits the measurement of the very weak magnetic fields emitted from the human brain due to intracellular neuronal currents. Current growth in MEG is dominated by multiple sensor arrays covering much of the head. These new large devices have primarily been developed and made commercially available by several companies including BTI[5] in the US, CTF[6] in Canada, and Neuromag[7] in Finland. Large projects are also in place in Japan[8]. These systems contain more than 100 sensors spaced at various intervals over the head using various configurations of magnetometers and gradiometers. The different designs available on the market are driven by factors such as detection efficiency, cost, and application.

We now present a completely novel whole-head SQUID array system using a superconducting imaging-surface gradiometer concept derived at Los Alamos. Preliminary tests have demonstrated higher performance, lower noise, and additional shielding of background fields while using simpler fabrication techniques than existing whole-head MEG systems, which should reduce production costs.

Theory

The superconducting imaging-surface gradiometer concept is described in detail in a companion paper in this conference[9]. A magnetic source causes Meissner currents in the superconductor that can be represented theoretically as an image source located behind the imaging surface. The SQUID magnetometer measures the flux resulting from the superposition of fields from both source and image. For a spherical imaging surface, the total field at the SQUID magnetometer is similar to that in an axial gradiometer located at the magnetometer. Magnetic field lines from sources outside the superconducting spherical imaging surface are excluded from the superconductor, causing the ambient field lines to wrap around the superconductor and shielding the sensors inside from those fields.

Van Hulsteyn showed that analytic expressions for superconducting imaging gradiometry[10] can only be derived for unconstrained geometry's (e.g. those without end). An analytic expression for the actual hemispherical shape of the whole-head image-surface must therefore assume a completely spherical shape. This assumption is justified for magnetic sources where the source-to-imaging-surface distance is much less than the distance from the source to the edge of the helmet. Thus, sources that are much closer to the imaging surface and/or the sensor than to the edge of the imaging surface will be adequately described by the analytic formalism of ref. [10]. We anticipate corrections will be required for sources close to the edge.

Finally, the superconducting imaging-surface theory holds only for an ideal superconductor, consequently any material properties, defects, or impurities that would cause appreciable regions of trapped flux, will distort the source image. Therefore, material choice, fabrication, and final treatment of the imaging surface must be performed with great care.

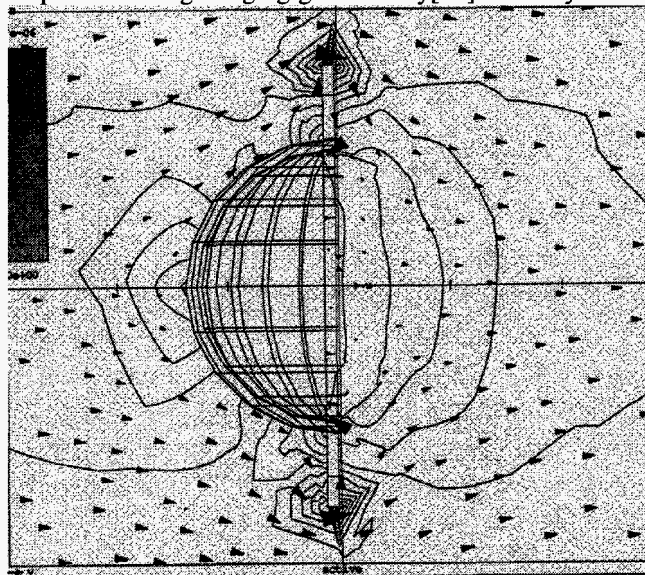


Figure 1. Finite element electromagnetic simulation of superconducting helmet in uniform ambient magnetic field. Arrow size is proportional to the field magnitude. Small or missing arrows inside of the hemisphere illustrates the screening effect of the superconducting helmet. Contours of equal flux density are also shown.

Method

A. Imaging-Surface Design

Finite element calculations to model the interaction between a superconducting hemisphere with a brim (or "helmet") and uniform ambient field have been carried out using the 3-D electromagnetic field modeling code OPERA[11]. The geometry of the model approximates the final design implemented for the whole-head system. Figure 1 shows the calculated magnetic field distribution around the geometry of the whole-head imaging surface for a normal incidence of an external (ambient) field. Arrow size in Fig. 1 is proportional to the field magnitude and small or missing arrows inside of the hemisphere illustrates the screening effect of the superconducting helmet. External fields were predicted to be screened (reduced) by a factor of 3500 at the inside apex of the hemisphere and approximately 2000 near the edge of the hemisphere. The large screening factor will be sufficient to reduce or possibly eliminate the need for a shielded room. The Meissner currents in the superconductor resulting from the excluded external fields only penetrate the outer surface of the superconducting helmet a few nanometers, thus they have no effect on the imaging properties of the inner surface. The SQUID sensors are located near the inner (concave) surface of the superconducting shield to produce the desired source images within the volume. Distant magnetic sources will not be imaged on the inner surface of the hemisphere and the helmet shields the vast majority of external fields from inside the hemisphere as shown in Fig. 1.

B. Dewar & Array Design

Photographs of the entire cryogenic column assembly and a close-up of the sensor array and imaging surface are shown in Figs. 2 and 3, respectively. The whole-head system dewar is complete, superinsulation and vapor cooled barrier installed, and boil-off rates measured. A new material, similar in composition to Corian®, was designed jointly by Los Alamos and DuPont for the SQUID sensor support structure. Macor®, a machinable ceramic, is the most common material used for this application in other systems. Although Macor is an excellent material for precision cryogenic applications, the raw material and precision machining costs are extremely high. Los Alamos and DuPont jointly developed a Corian-like plastic composite with the material properties important for a precision cryogenic application including material integrity under thermal cycling, isotropic thermal expansion coefficient, and the ability to precisely machine the material. The thermal expansion coefficient of the Corian-like plastic is much smaller than most plastics, though it is larger than Macor. Unlike Macor, the new material is readily machined to high tolerance and the raw material cost is quite small.

Finite element stress calculations were performed throughout the dewar design process to assure safety requirements were met. The helium boil-off rate for the dewar is acceptable with more than a five day liquid helium hold time without a column. The dewar column insert was designed to minimize heat transferred to the liquid helium, minimize RF interference to SQUID leads, minimize eddy current effects, and adequately support the SQUID and imaging surface helmet. The column has been fabricated and ten SQUID sensors installed for preliminary data acquisition.

The completed system including dewar, column and ten installed sensors (Fig. 2) has been operating for numerous helium fillings without failure. No indication of eddy currents in the RF shield have been observed. Improvements on vapor flow through the dewar insert are currently underway to increase dewar hold time. A close-up photograph of the Corian-like support structure with ten SQUIDs installed and niobium helmet is shown in Fig. 3.

A new thin-film button SQUID was specifically designed for use in image-surface systems by Conductus, Inc. in collaboration with and under contract to Los Alamos. Both the SQUID circuit and superconducting pickup loop are integrated on a single monolithic device using a niobium lithographic process. Details are presented in the companion paper at this conference[9].

The button SQUID-magnetometer sensors, approximately 1.2 cm in diameter, are each mounted on the end of a precision machined Corian-like mounting tube that is inserted into the support structure. The mounting tubes are positively seated against the imaging surface thereby precisely defining the sensor orientation and baseline. Each sensor is located very close to the inside

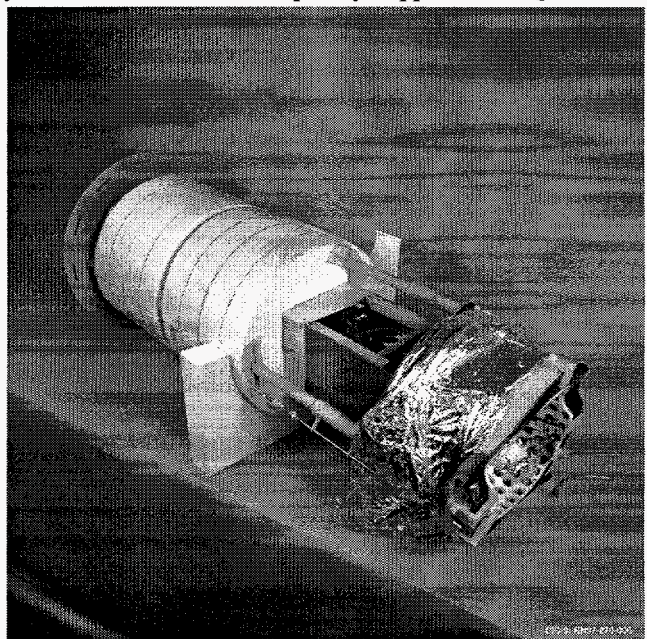


Figure 2. Photograph of the entire whole-head column assembly with a portion of the rf-shielding and interior superinsulation (used for additional rf-shielding) pulled back. Telescoping supports attach the imaging-surface and sensor array to the top plate of the column.

dewar wall while the imaging surface is perfectly hemispherical. Consequently, the tubes (and sensor baselines) vary in length. This design was chosen to place the sensors as close to the magnetic sources (subject head) as possible while maintaining a spherical imaging surface that greatly simplifies machining and modeling efforts. In practice, individual sensor calibration parameters for the varying baselines will be measured by a method of phantom calibrations and used in a fast table look-up algorithm during data analysis.

Both the lead and niobium superconducting surfaces were fabricated into a roughly 12 cm radius hemispherical shape. A final machining process assured a hemispherical shape (to a $25\mu\text{m}$ tolerance) and extremely fine finish ($<1\mu\text{m}$ finish) to the imaging surface. The lead helmet was fabricated using significantly thicker stock (0.25 inch) to assure stability and strength of the material. Initial testing of the niobium and lead helmets is described below.

Active background rejection will be implemented to supplement the screening effect of the superconducting imaging surface. Background magnetometers, located at intervals around the outer surface of the hemisphere, will measure the ambient vector field distribution outside the imaging surface while being highly screened from the sources of interest inside the helmet.

A detailed study of the electronics and timing required to operate these hardware gradiometers has recently been completed by Espy[12]. The critical timing techniques derived from this work will be used to further increase the background rejection for the whole-head system, reducing the need for a shielded room.

Results

Sensor noise and background field sensitivity measurements for ten sensors in the whole-head system have been completed for both the niobium and lead imaging surfaces. The ten SQUID sensors were initially placed in a cross pattern with six along the direction from the back edge of the system towards the apex and the other four crossing the pattern of the first six. This pattern permitted testing of sensors as a function of their position relative to the imaging helmet edge. A small magnetic dipole coil was used to assure that each sensor was working and to measure the noise and sensitivity characteristics of the ten sensors. SQUID sensor calibrations are only approximate because the dipole position relative to the sensors was uncertain due to thermal contraction of components during cool down. We observed noise levels of $12\text{fT}/\sqrt{\text{Hz}}$ at 10 Hz and $10\text{fT}/\sqrt{\text{Hz}}$ at 100 Hz within a shielded chamber and $\sim 1\text{pT}/\sqrt{\text{Hz}}$ unshielded in our very (electrically) noisy laboratory for the SQUID sensor nearest the helmet brim.

The majority of measurements were performed in an unshielded environment for both the niobium and lead helmets. Background (primarily 60Hz line frequency) and RF field attenuation was sufficient in all cases to enable all SQUIDs to lock in the extremely noisy environment of our laboratory. We observed a 23Hz magnetic dipole source with 100fT at 3cm field using this preliminary configuration. A Stanford Research SRS-650 spectrum analyzer was used with 1 second averaging to obtain a signal-to-noise ratio of ~ 3 .

The background screening factor was measured by operating the whole-head system inside a 2.5 x 2.5 meter set of Helmholtz coils activated at several frequencies to produce a uniform field. The superconducting helmet was oriented at approximately a 20° angle (tilted back) relative to the field lines produced by the Helmholtz coils. The screening factor is the ratio of the field outside the helmet to that detected at the sensors inside the imaging surface. We observed screening factors at 60° inclination of ~ 400 for the SQUID sensor in the niobium helmet and ~ 1800 at the same sensor location when using the lead helmet. One explanation for this difference is the existence of significantly more and/or larger regions of normal material in the niobium helmet, a type II superconductor, caused by material inclusions and stress perturbations, than are present in the lead. The measured screening factor inside the lead imaging-surface helmet as a function of inclination angle is plotted in Fig. 4 for two methods of cooling the system through the superconducting transition: 1) with the dewar in the unshielded laboratory and 2) with the dewar shielded inside a mu-metal can. The data clearly show a substantial improvement in shielding factor for the helmet when it is cooled in a well-shielded environment. This observation indicates the lead helmet is not an ideal superconductor and likely has inclusions in the material that are causing significant flux to be trapped when the helmet is cooled in the earth's field. The trapped flux acts as a flux leak through the helmet and is also likely to cause aberrations in the imaging performance of the helmet. We are currently building a new lead helmet that will have far better superconducting properties. The multiple points for both curves at 40° inclination result from four sensors at that inclination due to the "cross" configuration.

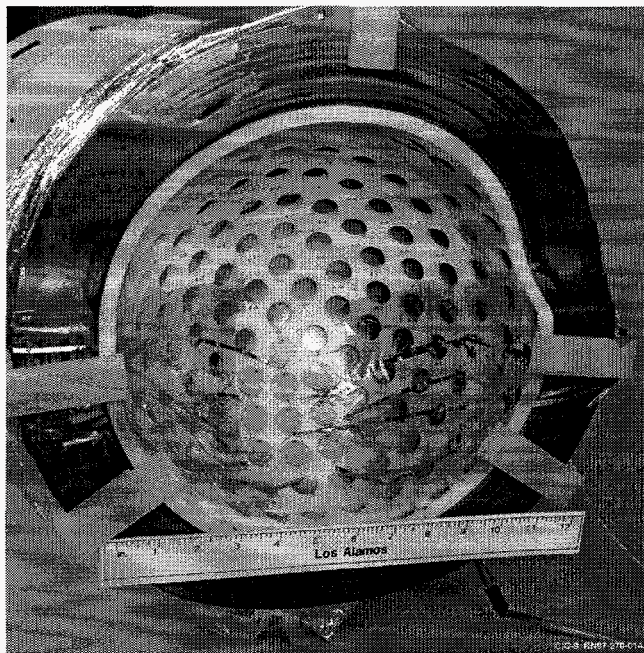


Figure 3. A close-up photograph of the niobium superconducting imaging-surface helmet, SQUID sensor array support structure, and ten of the total 155 integrated SQUID magnetometers mounted. The niobium was replaced by a higher-quality lead helmet for measurements reported in this paper.

Screening factors for the lead helmet are less than predicted by theoretical calculations. Finite element model calculations predicted screening factors of 3500 at the apex of a superconducting helmet to around 2000 near the edge. This apparent discrepancy largely results from the fact that the separation between the sensors and the imaging surface in the finite element model was less than actual experimental values. Other possible contributors include that the absolute calibration of the SQUID sensors has not been performed, and that the lead imaging surface has nonsuperconducting regions.

Finally, the measured response of the imaging-surface SQUID sensors to magnetic dipole sources agreed very well with the predicted values using the analytic formalism developed in ref. [10] for sensors that were closer to the magnetic source than the edge of the imaging surface[9]. Variation from predicted values increased for sensors near the imaging-surface edge (Fig. 5, SQUIDs 7,8). The largest discrepancy, however, was observed for SQUID 5, which was closer to the source coil than SQUIDs 7 or 8. We hypothesize SQUID 5 was closest to a non-superconducting inclusion as discussed above. The agreement with theory is none-the-less very good and could, if a higher quality imaging surface were not available, be corrected by using a calibration table. A careful phantom study will be performed to correlate sensor response with source position. This data will be used to construct a calibration table for all sensors, particularly those close to the edge, to correct sensor data.

Conclusion

We have demonstrated the viability of using superconducting imaging-surface gradiometry to build a whole-head SQUID array MEG system. The superconducting imaging theory for imaging surfaces has been validated and lead was found to perform far better than niobium. New integrated SQUID magnetometers, coupled with the imaging-surface provide exceptional performance. Shielding of ambient fields inside the helmet, combined with previously reported hardware gradiometry methods[12] should provide total shielding of $>10^5$ for frequencies up to 1kHz. This level of shielding should enable superconducting imaging-surface MEG systems to be used with little or no additional shielding, greatly reducing future system costs to the research and clinical communities.

References

- [1] Cohen, D., 1968, "Magnetoencephalography: Evidence of magnetic fields produced by alpha-rhythm currents", *Science*, **161**, 784-786
- [2] Cohen, D., 1972, "Magnetoencephalography: Detection of the brain's electrical activity with a superconducting magnetometer", *Science* **175**, 664-666
- [3] Brenner, D., Williamson, S. J., Kaufman, L., 1975 "Visually evoked magnetic fields of the human brain", *Science* **190**, 480-482
- [4] Josephson, B. D., 1962, "Possible new effects in superconducting tunneling", *Phys. Lett.* **1**, 251-253
- [5] Biomagnetic Technologies Inc. (BTI), 1995, 9727 Pacific Heights Blvd. San Diego, CA, 92121-3719
- [6] CTF Systems Inc., 1995, #15-1750 McLean Avenue, Port Coquitlam. B. C. V3C 1M9, Canada
- [7] Neuromag Ltd., 1995, c/o Low Temperature Laboratory, Helsinki University of Technology, 02150 Espoo, Finland
- [8] Superconducting Sensor Laboratory of Japan (SSL) 1995, 1-6-5 Higashi-Nihonbashi, Chuo-ku, Tokyo 103, Japan
- [9] Kraus, Jr., R.H., Flynn, E.R., Espy, M.A., Matlachov, A., Overton, W., Peters, M.V., Ruminer, P.A., "First Results for a Superconducting Imaging-Surface Sensor Array for Magnetocardiography," these proceedings.
- [10] van Hulsteyn, D. B., Petschek, A. G., Flynn, E. R., and Overton, W. C. Jr., 1995, "Superconducting Imaging Surface Magnetometry", *Rev. Sci. Instrum.* **66**, 3777-3784
- [11] Vector Fields, Inc., 1996, OPERA Electromagnetic Modeling Code.
- [12] Espy, M. A., Flynn, E. R., Kraus, R., and Matlachov, A., "Two methods for a first order hardware gradiometer using two HTS SQUIDs," *Rev. of Sci. Instr.*, **69**, No. 1, 123-129 (1998)

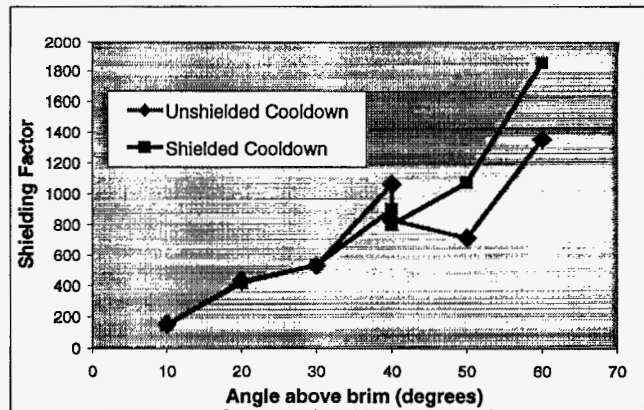


Figure 4. Comparison plot of whole-head shielding factor for lead superconducting imaging-surface cooled in ambient field (squares) and in absence of field (diamonds).

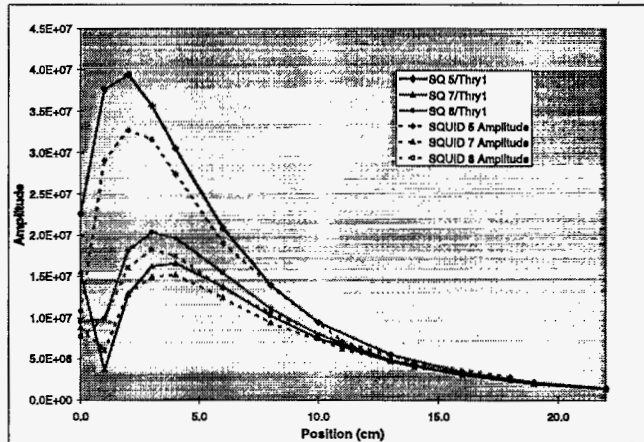


Figure 5. Comparison plot of measured gradiometer response and theoretical predictions using the analytic formalism of ref. 10 for SQUID sensors located both far from the magnetic dipole source and rather close to the imaging-surface edge.